INTERNATIONAL ATOMIC ENERGY AGENCY
UNITED NATIONS EDUCATIONAL, SCIENTIFIC AND CULTURAL ORGANIZATION
INTERNATIONAL CENTRE FOR THEORETICAL PHYSICS
I.C.T.P., P.O. BOX 586, 34100 TRIESTE, ITALY, CABLE: CENTRATOM TRIESTE

H4.SMR/854-23

College on Computational Physics

15 May - 9 June 1995

Ab initio Molecular Dynamics

V. Kumar

Indira Gandhi Centre for Atomic Research
Kalpakkam, India

AB INITIO MOLECULAR DYNAMICS

VIJAY KUMAR

MATERIALS SCIENCE DIVISION, INDIRA GANDHI CENTRE FOR ATOMIC RESEARCH, KALPAKKAM - 603102.

PLAN

INTRODUCTION

DENSITY FUNCTIONAL THEORY

PSEUDOPOTENTIALS

CAR-PARRINELLO METHOD

SOME APPLICATIONS

WORK AT ICTP + SISSA

IN COLLABORATION WITH R. CAR AND V. SUNDARARAJAN

CLASSICAL MOLECULAR DYNAMICS

USES EMPIRICAL POTENTIALS FOR INTERATOMIC INTERACTIONS BETWEEN ATOMS WHICH IS QUANTUM MECHANICAL.

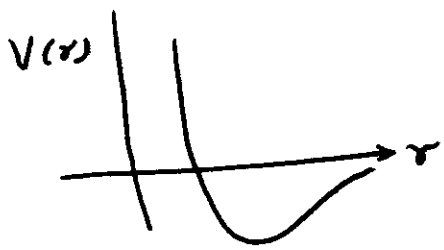

THE EMPIRICAL POTENTIALS ARE GENERATED BY FITTING TO SOME PROPERTIES OF KNOWN STRUCTURES OF A MATERIAL

EMPIRICAL POTENTIALS NOT TRANSFERABLE AND THEREFORE CAN NOT BE USED FOR UNKNOWN STRUCTURES SUCH AS CLUSTERS, AMORPHOUS MATERIALS, SURFACES (RECONSTRUCTION), CHEMICAL REACTIONS AND MD IN GENERAL, ARTIFICIAL STRUCTURES ETC. MAGNETIC PROP., BONDING CHANGES

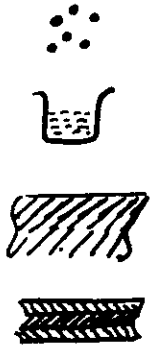

ENERGY DIFFERENCES SMALL
COHESIVE ENERGY ~ eV
STRUCTURAL ENERGY DIFFERENCE ~ 0.1 eV
ORDERING ENERGIES ~ 0.01 eV
PHONONS, MAGNETIC ORDERING ~ 0.01 eV
TOTAL ENERGY ~ 100 - 10000 eV

$\Rightarrow$ DEMANDS VERY HIGH PRECISION

AN IMPORTANT MILESTONE

DENSITY FUNCTIONAL THEORY (964-65

Hohenberg + Kohn, PR 136, B864

Kohn + Sham, PR 140, A1133

REALISTIC CALCULATIONS BECAME POSSIBLE

THE BASIC PROBLEM ARISES FROM THE MANY BODY TERM IN

$$H = -\sum_{i}^{\text{Particles}} \left(\frac{\hbar^2}{2m} \vec{\nabla}_i^2 + \sum_{I}^{\text{ions}} \frac{Z_I e^2}{|\vec{r}_i - \vec{R}_I|} \right) + \frac{1}{2} \sum_{\substack{i,j \\ i \neq j}} \frac{e^2}{|\vec{r}_i - \vec{r}_j|}$$

SCHRÖDINGER EQN. $H\Psi = E\Psi$

$\Psi \equiv \Psi(\vec{r}_1, \vec{r}_2, \ldots \vec{r}_N)$, N PARTICLES

ONE NEED TO SOLVE A SYSTEM OF 3N VARIABLES

HARTREE APPROXIMATION

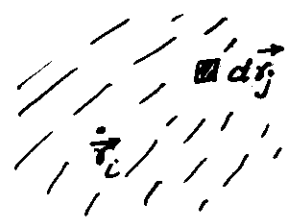

MEAN FIELD THEORY

$$V^{ee}(\vec{r}_i) = e^2 \int \frac{|\psi(\vec{r}_j)|^2}{|\vec{r}_i - \vec{r}_j|} d\vec{r}_j$$

AND PROBLEM REDUCES TO SOLUTION OF N <u>SINGLE PARTICLE</u> EQUATIONS:

$$\left(-\frac{\hbar^2}{2m} \vec{\nabla}^2 - \sum_I \frac{Z_I e^2}{|\vec{r} - \vec{R}_I|} + e^2 \int \frac{|\psi(\vec{r}')|^2}{|\vec{r} - \vec{r}'|} d\vec{r}' \right) \psi(\vec{r}) = \varepsilon \psi(\vec{r})$$

NEED SELF-CONSISTENT SOLUTION

DOES NOT INCLUDE CORRELATED MOTION OF $\bar{e}$

$\Rightarrow$ $\bar{e}$ SPENDS MORE TIME IN THE IMMEDIATE VICINITY OF EACH OTHER THAN IT IS ACTUALLY THE

AN OBSERVABLE QUANTITY (SAY $\rho(\vec{r})$) MUST BE SYMMETRIC WITH RESPECT TO INTERCHANGE OF COORDINATES

$$|\Psi(x_1, x_2, \cdots x_N)|^2 = |\Psi(x_2, x_1, \cdots x_N)|^2$$
$$= |P\Psi(x_1, x_2, \cdots x_N)|^2$$

x INCLUDES SPIN

OR $\Psi(x_2, x_1, \cdots x_N) = P_{12}\Psi(x_1, x_2, \cdots x_N)$

$$P_{12}P_{21} = e^{2i\theta_{12}} = 1 \quad \text{or} \quad e^{i\theta_{12}} = \pm 1$$

SO $\Psi(x_2, x_1, \cdots x_N) = \pm\Psi(x_1, x_2, \cdots x_N)$.

PAULI PRINCIPLE $\Rightarrow$ WAVE FUNCTION ANTI-SYMMETRIC $\Rightarrow$ HARTREE-FOCK

$$\Psi = \sum_P a_P P \phi_1(x_1)\phi_2(x_2)\cdots\phi_N(x_N)$$

$\Rightarrow$ SLATER DETERMINANT

$$\Psi = \begin{vmatrix} \phi_1(x_1) & \phi_1(x_2) & \cdots & \phi_1(x_N) \\ \phi_2(x_1) & \phi_2(x_2) & \cdots & \phi_2(x_N) \\ \phi_3(x_1) & \phi_3(x_2) & \cdots & \phi_3(x_N) \\ \vdots & \vdots & & \vdots \\ \phi_N(x_1) & \phi_N(x_2) & \cdots & \phi_N(x_N) \end{vmatrix}$$

OR $\phi_1 = \phi_2$

IF $x_i = x_j$, $\Rightarrow \Psi = 0$ & INTERCHANGE OF x_1 and x_2 CHANGES SIGN OF Ψ.

$$E = \langle\Psi|H|\Psi\rangle$$

$$E = \sum_{i=1}^{N} \int \phi_i^*(x_i) \left[-\frac{\hbar^2}{2m} \nabla_i^2 - \sum_I \frac{Z_I e^2}{|\vec{r}_i - \vec{R}_I|} \right] \phi_i(x_i)\, dx_i$$

$$+ \frac{1}{2} \sum_{\substack{i,j \\ i \neq j}} \iint \frac{e^2}{r_{ij}} |\phi_i(x_i)|^2 |\phi_j(x_j)|^2 dx_i\, dx_j$$

$$- \frac{1}{2} \sum_{\substack{i,j \\ i \neq j}} \iint \frac{e^2}{r_{ij}} \phi_i^*(x_j)\, \phi_j^*(x_i)\, \phi_i(x_i)\, \phi_j(x_j)\, dx_i\, dx_j$$

⇓ SUM OVER SPIN VARIABLES

$$- \frac{1}{2} \sum_{\substack{i,j \\ i \neq j}} \iint \frac{e^2}{r_{ij}} \phi_i^*(\vec{r}_j)\, \phi_j^*(\vec{r}_i)\, \phi_i(\vec{r}_i)\, \phi_j(\vec{r}_j)\, d\vec{r}_i\, d\vec{r}_j$$

11 SPINS $\qquad$ $i=j$ CANCELS

$$E = \sum_i \int \phi_i^*(\vec{r}_i)\, H_i\, \phi_i(\vec{r}_i)\, d\vec{r}_i$$

$$H_i = -\frac{\hbar^2}{2m} \nabla_i^2 - \sum_I \frac{Z_I e^2}{|\vec{r}_i - \vec{R}_I|} + e^2 \sum_j \int \frac{|\psi_j(\vec{r}_j)|^2}{r_{ij}} d\vec{r}_j$$

$$- e^2 \sum_{\substack{j \\ \text{SPIN } j = \text{SPIN } i}} \int \frac{\psi_j^*(\vec{r}_j)\, \psi_i(\vec{r}_j)\, \psi_j(\vec{r}_i)}{r_{ij}\, \psi_i(\vec{r}_i)} d\vec{r}_j$$

EXCHANGE TERM ARISING FROM A +ve CHARGE DISTRIBUTION

$\Longrightarrow$ EXCHAGE HOLE OF DENSITY

$$e \sum_{\substack{j \\ \text{SPIN } j = \text{SPIN } i}} \frac{\psi_j^*(\vec{r}_j)\, \psi_i(\vec{r}_j)\, \psi_j(\vec{r}_i)}{\psi_i(\vec{r}_i)} \quad \text{at } \vec{r}_j$$

TOTAL CHARGE IN THIS HOLE IS

$$e \sum_{\substack{j \\ \text{spin } j = \text{spin } i}} \int \frac{\psi_j^*(\vec{r}_j)\, \psi_i(\vec{r}_j)\, \psi_j(\vec{r}_i)}{\psi_i(\vec{r}_i)} d\vec{r}_j = e$$

ALSO FOR $\vec{r}_i = \vec{r}_j$, THIS IS EQUAL TO $e \sum_j^N |\psi_j(\vec{r}_i)|^2$

HARTREE-FOCK IGNORES PROPER COULOMB CORRELATIONS

BUT INCLUDES CORRELATIONS AMONG THE POSITIONS OF ELECTRONS WITH PARALLEL SPINS ONLY, WHICH ARISE DUE TO PAULI PRINCIPLE. IT NEGLECTS CORRELATIONS BETWEEN TWO ELECTRONS WITH ANTIPARALLEL SPINS.

ALL CORRELATIONS NOT INCLUDED IN THE EXCHANGE TERM ARE REFERRED TO AS CORRELATIONS AND THE ENERGY AS CORRELATION ENERGY.

HOHENBERG AND KOHN:

ELECTRONIC DENSITY $n(\vec{r})$ THE IMPORTANT QUANTITY. (BASIC VARIABLE)

Let $H = T + V + U$

T: KINETIC ENERGY

V: EXTERNAL POT.

U: $\bar{e}$-$\bar{e}$ INT.

THEOREM

$v(\vec{r})$ AND Ψ ARE UNIQUELY DETERMINED BY THE KNOWLEDGE OF THE DENSITY DISTRIBUTION $n(\vec{r})$ WITHIN A TRIVIAL ADDITIVE CONSTANT.

PROOF

ASSUME A DIFFERENT POTENTIAL $v'(\vec{r})$ WITH A GROUND STATE Ψ' THAT GIVES RISE TO THE SAME DENSITY $n(\vec{r})$

THEN UNLESS $v'(\vec{r}) - v(\vec{r}) = \text{CONST.}$ $\Psi' \neq \Psi$ SINCE THESE STATES ARE EIGENSTATES OF DIFFERENT HAMILTONIANS

Ψ , H, E $\quad n(\vec{r})$

Ψ', H', E' $\quad n(\vec{r})$

THEN $\quad E = \langle \Psi | H | \Psi \rangle < \langle \Psi' | H | \Psi' \rangle = \langle \Psi' | H' + V - V' | \Psi' \rangle$

OR $\quad E < \langle \Psi' | H' | \Psi' \rangle + \langle \Psi' | V - V' | \Psi' \rangle$

$$E < E' + \langle \Psi' | V - V' | \Psi' \rangle$$

$$< E' + \int \{ v(\vec{r}) - v'(\vec{r}) \} n(\vec{r}) \, d\vec{r}$$

$$E' < E + \int \{ v'(\vec{r}) - v(\vec{r}) \} n(\vec{r}) \, d\vec{r}$$

ADD

$$E + E' < E + E'$$

SO THE ASSUMPTION THAT THE DENSITY IS THE SAME, WAS WRONG

NOW DEFINE

$$F[n(\vec{r})] = \langle \Psi | T + U | \Psi \rangle$$

IT CONTAINS ALL INTERACTIONS

$$E_v[n(\vec{r})] = \int v(\vec{r}) \, n(\vec{r}) \, d\vec{r} + F[n(\vec{r})]$$

Let

$$G[n] = F[n] - \frac{1}{2} \int \frac{n(\vec{r}) \, n(\vec{r}')}{|\vec{r} - \vec{r}'|} \, d\vec{r} \, d\vec{r}'$$

$$= T_s[n] + E_{xc}[n]$$

WHERE $T_s[n]$ IS THE K.E. OF A NON-INTERACTI ELECTRON GAS OF DENSITY $n(\vec{r})$. $E_{xc}[n]$ IS THE EXCHANGE CORRELATION ENERGY.

$$E_v[n(\vec{r})] = T_s[n(\vec{r})] + \int v(\vec{r})\, n(\vec{r})\, d\vec{r}$$

$$+ \frac{1}{2}\int \frac{n(\vec{r})\, n(\vec{r}')}{|\vec{r}-\vec{r}'|}\, d\vec{r}\, d\vec{r}' + E_{xc}[n(\vec{r})]$$

THIS SIMILAR TO THE HARTREE FORM EXCEPT E_{xc}.

TO OBTAIN THE GROUND STATE, MINIMIZE E_v SUBJECT TO

$$\int n(\vec{r})\, d\vec{r} = N$$

$$\Rightarrow \frac{\delta T_s}{\delta n(\vec{r})} + \phi(\vec{r}) + v_{xc}(\vec{r}) - \mu = 0$$

Lagrange Multiplier

$$\phi(\vec{r}) = v(\vec{r}) + \int \frac{n(\vec{r}')}{|\vec{r}-\vec{r}'|}\, d\vec{r}'$$

$$v_{xc}(\vec{r}) = \frac{\delta E_{xc}}{\delta n(\vec{r})}$$

IF v_{xc} IS NOT THERE, THEN THE ABOVE EQUATIONS ARE HARTREE EQUATIONS. SO WE CAN WRITE

$$\left[-\frac{1}{2}\nabla^2 + v_{eff}(\vec{r})\right]\psi_i(\vec{r}) = \varepsilon_i\, \psi_i(\vec{r})$$

$$v_{eff}(\vec{r}) = \phi(\vec{r}) + v_{xc}(\vec{r})$$

$$n(\vec{r}) = \sum_{i=1}^{\text{occupied}} f_i\, |\psi_i(\vec{r})|^2$$

KOHN - SHAM EQUATIONS

v COULD BE ALL ELECTRON OR PSEUDOPOTENTIAL

E_{xc} IS STILL PROBLEMATIC, AND APPROXIMATE FORMS ARE USED. THE MOST COMMON IS THE LOCAL DENSITY APPROXIMATION(LDA)

$$E_{xc}[n(\vec{r})] = \int \epsilon_{xc}(n(\vec{r}))\, n(\vec{r})\, d\vec{r}$$

$\epsilon_{xc}(n(\vec{r}))$ IS THE EXCHANGE CORRELATION ENERGY PER PARTICLE FOR A UNIFORM ELECTRON GAS OF DENSITY $n(\vec{r})$. THERE ARE SEVERAL RESULTS AVAILABLE FOR ϵ_{xc}.

$$\epsilon_{xc}(n) = -\frac{0.458}{r_s} - 0.0666\, G\left(\frac{r_s}{11.4}\right)$$

$$G(x) = \frac{1}{2}\left[(1+x^3)\log(1+x^{-1}) - x^2 + \frac{x}{2} - \frac{1}{3}\right]$$

LDA HAS YIELDED VERY GOOD RESULTS.

HOWEVER, IT GENERALLY GIVES OVERBINDING SHORTER BOND LENGTHS.

FOR SEMICONDUCTORS THE GAP IS UNDERESTIMATED BY UPTO 40–50%.

WORKS BADLY FOR VAN DER WAALS BONDED SYSTEMS.

HOWEVER THE GENERAL TRENDS COMES OUT VERY WELL.

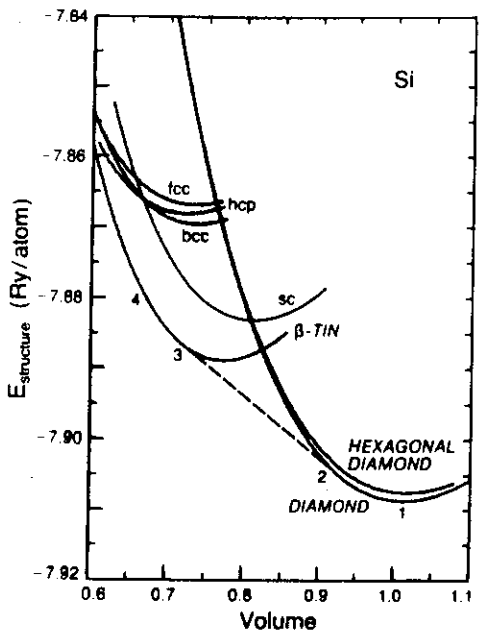

Fig. 13. Equation of state for silicon, calculated by Yin and Cohen [99] for seven crystal structures. The slope of the dashed line gives the critical pressure for transformation from the diamond to the β-tin structure.

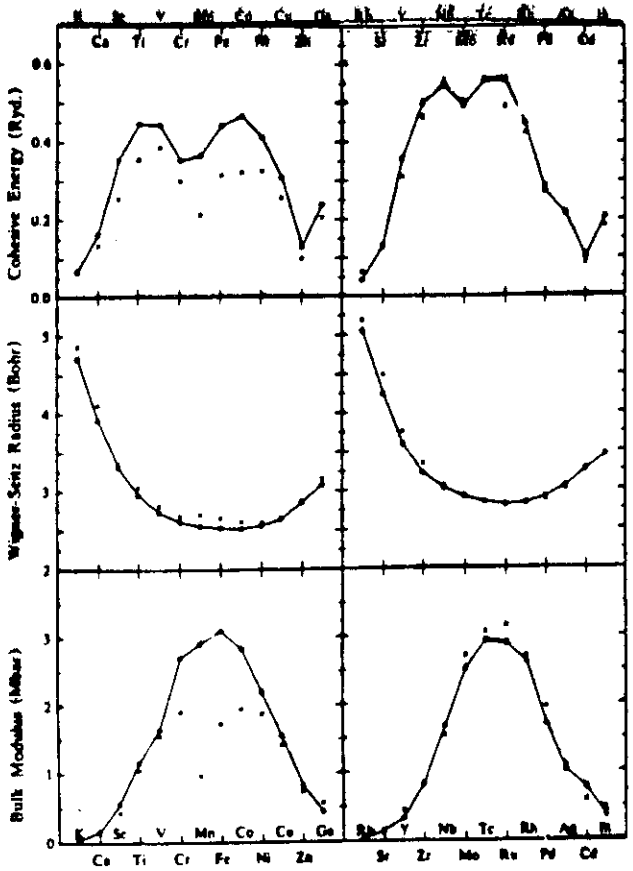

FIGURE 17. Comparison with experiment of ground-state properties given by self-consistent-field calculations based on the local-density approximation to density-functional theory. The left- and right-hand sides of the figure present results for the 3*d* and 4*d* transition series, respectively. The middle row gives equilibrium atomic volumes or lattice constants in terms of the corresponding Wigner–Seitz radii. The upper row gives cohesive energies and the bottom row gives bulk moduli. The calculations are described in Ref. 90; they employ the "muffin-tin" approximation, but are otherwise completely parameter-free. Spin-polarization effects have been included in the free-atom calculations required for the specification of the cohesive energy. These effects have not been included in the description of the solids which order magnetically. Measured values are indicated by crosses, calculated values by connected points. References to the experimental work can be found in Ref. 90.

restricted to molecules comprised of very light atoms, so that no assessment is provided of the ability of the local-density approximation to describe, for example, Π-bonded systems or transition-metal systems involving localized *d* electrons. The diatomic molecules formed from atoms in the first row of the Periodic Table have been studied by three groups[145–148] using successively more accurate numerical methods. These calculations taken together provide a very encouraging assessment of the accuracy of the local-density approximation.

The binding energy of the H_2 molecule $[E(H_2)-2E(H)]$ as a function of internuclear separation is shown in Fig. 9. The figure compares essentially exact results for the binding curve[146,147] with those obtained using different calculational procedures (with and without the use of the muffin-tin approximation, for example) and using different approximate treatments of exchange and correlation (local-density,[142] $X\alpha$,[148] and Hartree–Fock[149]).

Three aspects of Fig. 9 warrant comment. First, the local-spin-density result is significantly more accurate than the Hartree–Fock and $X\alpha$ results. Second, the local-spin-density results differ from the exact result by only 0.1 eV. Third, as mentioned above, the binding energy is significantly corrupted by use of the muffin-tin approximation (the result in Fig. 9 labeled MS–$X\alpha$).

Consider now applications of the local-spin-density approximation to more complicated molecules, in which the presence of core states requires

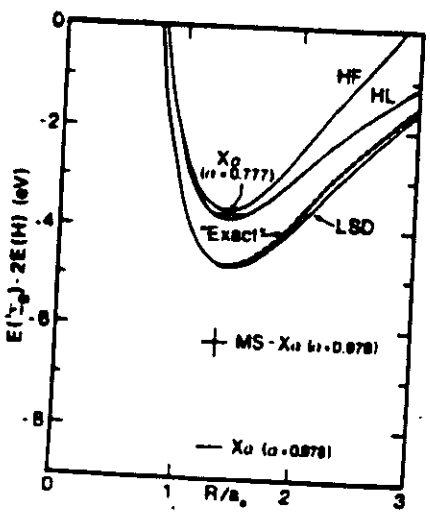

FIGURE 9. Comparison of calculated binding energies for molecular H_2. For H_2, both the exact result (Refs. 146 and 147) and the exact local-spin-density result (Ref. 142) are available both for mutual comparison and for comparison with results obtained using more approximate methods. The Hartree–Fock (HF) results are those of Ref. 149 and the $X\alpha$ results are those of Ref. 148. The MS–$X\alpha$ result (Ref. 148) was obtained using the muffin-tin approximation.

more elaborate
than were adequ
performed by O.
results for the fi
free local-spin-de
trend across the
across the series
atomic number
17 below.) This
gressive filling of

Additional i
lecular bonding

FIGURE 10. Comp
first-row diatomic
mation. The proper
nuclear separation
143) employ the lin
sured values are the

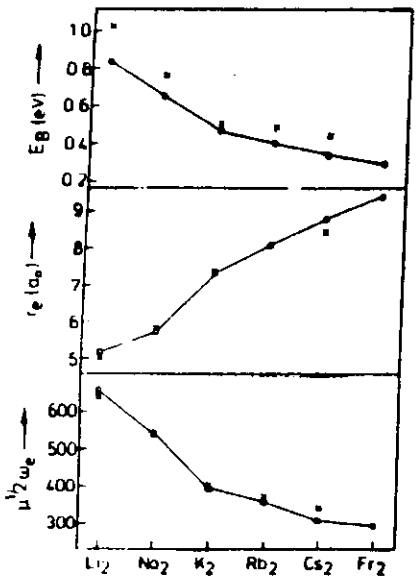

FIGURE 13. Comparison of measured and calculated molecular bonding properties of the alkali dimers. Shown are the binding energy E_B, the equilibrium internuclear separation r_e, and the weighted vibration frequency $\mu^{1/2}\omega_e$, where μ is the reduced mass. The calculated values are those of Ref. 160, where references to the experimental work can also be found.

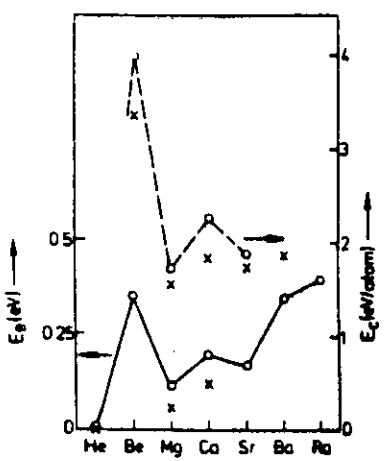

FIGURE 14. Comparison of molecular and solid-state bonding properties for the group II elements. The molecular calculations are described in Ref. 159; the cohesive-energy calculations are those of Ref. 90. The measured cohesive energies (crosses) are from Ref. 162. The measured binding energy for Mg_2 is from Ref. 163; that for Ca_2 is from Ref. 164. Both the cohesive energy and the molecular-bond energy for He can be considered to be zero in this context.

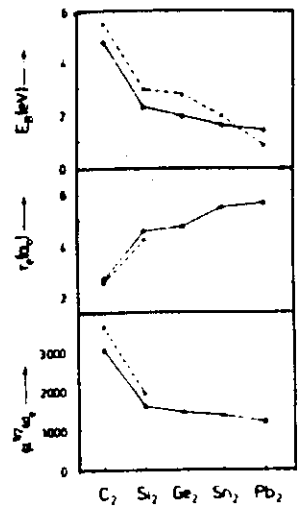

FIGURE 15. Comparison of measured (crosses) and calculated (circles) molecular bonding properties of the group IV dimers. Shown are the binding energy E_B, the equilibrium internuclear separation r_e, and the weighted vibration frequency $\mu^{1/2}\omega_e$, where μ is the reduced mass. The calculations are described in Ref. 161, where references to the experimental work can also be found.

the 3*d* levels are unoccupied and their contribution to bonding is relatively large because they lie relatively low in energy and, therefore, contribute readily to the polarization of the atom. In Rb, on the other hand, the presence of the 3*d* levels in the core pushes the unoccupied atomic 4*d* levels to relatively higher energies. At the same time, the penetration of the 3*d* core shell in Rb by the 4*s* electrons lowers their energy, further separating them from the unoccupied polarization levels.

The most direct manifestation of this effect is a pairing of the valence orbitals of the free atom. Harris and Jones have plotted these orbitals for the atoms in groups $I^{(89)}$ $II^{(89)}$ and $IV^{(160)}$ of the Periodic Table; we show in Fig. 12 those for group II atoms. Consider, as an example, the *s* orbitals of the group II atoms (Fig. 12a). Without the effect described above, the valence orbitals would become steadily more delocalized as we move down a column of the Periodic Table, because the attraction due to the increasing nuclear charge does not completely compensate for the repulsion of the orthogonality requirement. We see in Fig. 12a that this steady progression is broken by the entry of the 2*p*, 3*d*, and 4*f* shells into the core. The 2*p* shell makes Mg similar to Be; the 3*d* shell makes Sr similar to Ca; and the 4*f* shell makes Ra similar to Ba. The molecular bonding properties (dissociation energy, bond length, and vibration frequency) are shown for groups $I^{(159)}$ and $IV^{(161)}$ dimers in Figs. 13 and 15.

PSEUDOPOTENTIALS:

FOR CHEMICAL BONDING AND RELATED PROPERTIES ONLY THE VALENCE ELECTRONS PLAY THE IMPORTANT ROLE. THE CORE ELECTRONS REMAIN NEARLY UNCHANGED.

$\Longrightarrow$ THROW AWAY THE CORE ELECTRONS.

THE VALENCE ELECTRON WAVE FUNCTIONS ORTHOGONAL TO THE CORE STATES $\rightarrow$ WIGGLE IN THE WAVE FUNCTION

CONSTRUCT ORTHOGONALIZED PLANE WAVES 1OPW;

$$|OPW\rangle_{\vec{k}} = |\vec{k}\rangle - \sum_c |c\rangle\langle c|\vec{k}\rangle$$

$$\langle c|\vec{k}\rangle = \frac{1}{\sqrt{\Omega}} \int \psi_c^*(\vec{r})\, e^{i\vec{k}\cdot\vec{r}}\, d\vec{r}$$

Let $P = \sum_c |c\rangle\langle c|$

THEN $|OPW\rangle_{\vec{k}} = (1-P)|\vec{k}\rangle$

CONSTRUCT LINEAR COMBINATION OF $|OPW\rangle$'s

$$\psi_{\vec{k}} = \sum_{\vec{G}} c_{\vec{k}+\vec{G}} (1-P)|\vec{k}+\vec{G}\rangle$$

THEN FROM $H\Psi = E\Psi$ WE GET

$$\sum_{\vec{G}} C_{\vec{k}+\vec{G}} H(1-P)|\vec{k}+\vec{G}\rangle = E_{\vec{k}} \sum_{\vec{G}} C_{\vec{k}+\vec{G}} (1-P)|\vec{k}+$$

Multiply on the left with $|\vec{k}+\vec{G}'\rangle$ to get

$$C_{\vec{k}+\vec{G}'} \frac{\hbar^2}{2m}|\vec{k}+\vec{G}'|^2 + \sum_{\vec{G}} C_{\vec{k}+\vec{G}} [\langle \vec{k}+\vec{G}'|V|\vec{k}+\vec{G}$$

(A) $$- E_c \langle \vec{k}+\vec{G}'|c\rangle\langle c|\vec{k}+\vec{G}\rangle]$$

$$= E_{\vec{k}} [C_{\vec{k}+\vec{G}'} - \sum_{\vec{G}} C_{\vec{k}+\vec{G}} \langle \vec{k}+\vec{G}'|P|$$
$$\vec{k}+\vec{G}\rangle$$

WHERE $H|c\rangle = E_c|c\rangle$ $|c\rangle$: CORE STATE

Let $$\varphi_{\vec{k}} = \sum_{\vec{G}} C_{\vec{k}+\vec{G}} |\vec{k}+\vec{G}\rangle$$

THEN (A) REDUCES TO

$$T\varphi_{\vec{k}} + W\varphi_{\vec{k}} = E_{\vec{k}}\varphi_{\vec{k}}$$

$$W = V(\vec{r}) + \sum_c (E_{\vec{k}} - E_c)|c\rangle\langle c|$$

IS THE PSEUDOPOTENTIAL

E_c MORE -ve THAN E_k's

$$\langle \varphi_{\vec{k}}|W|\varphi_{\vec{k}}\rangle = \langle \varphi_{\vec{k}}|V|\varphi_{\vec{k}}\rangle + \sum_c (E_{\vec{k}} - E_c) \cdot |\langle \varphi_{\vec{k}}|c\rangle|^2$$

$\Rightarrow$ W IS A WEAKER POTENTIAL THAN V.

BUT THE PSEUDO WAVE FUNCTION THUS CONSTRUCTED i.e. φ_R DOES NOT MATCH WITH THE EXACT WAVE FUNCTION. THE EIGEN VALUES ARE CORRECT.

PROBLEMS IN USING IT FOR SURFACES, MOLECULES, CLUSTERS ETC.

⇓

NORM CONSERVING PSEUDOPOTENTIALS.

Bachelet et al

THE WAVEFUNCTION AND THE POTENTIAL SAME AS ALL ELECTRON WF AND POT.

BEYOND A CERTAIN RADIUS. i.e. ~~THE~~ NORM OF THE PSEUDO WF IS ~~THE~~ SAME AS ALL ELECTRONS BEYOND THIS RADIUS.

THE EIGEN VALUES SAME AS ALL ELECTRO

VERY SUCCESSFUL.

TRANSFERABLE.

CONSTRUCTION OF PSEUDOPOTENTIAL

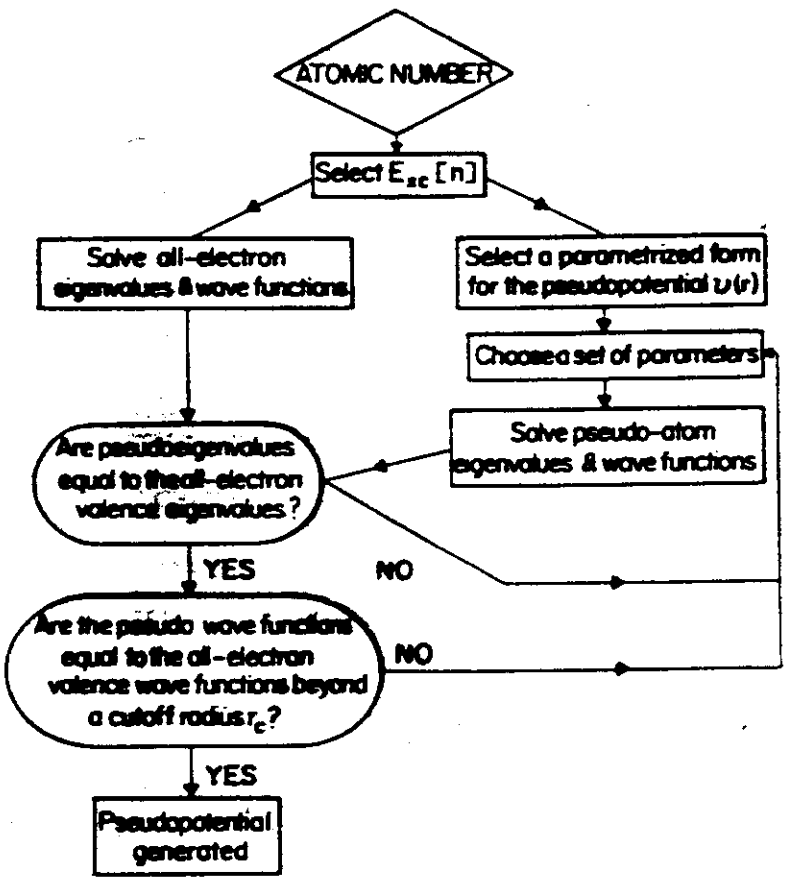

FIG. 6. Flow chart describing the construction of an ionic pseudopotential for an atom.

Norm Conserving pseudopotentials

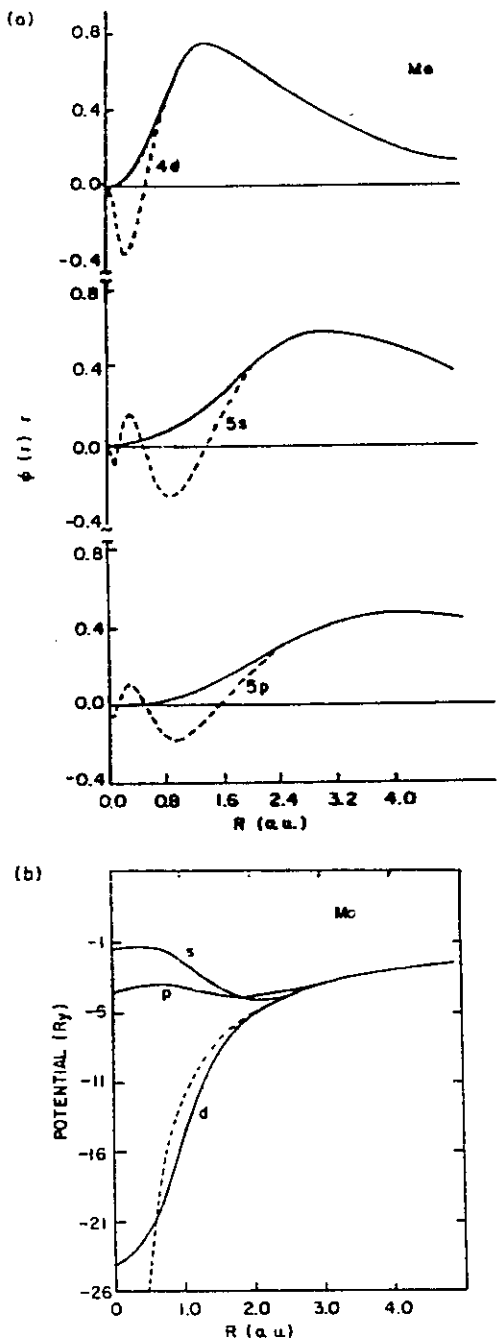

FIG. 1. (a) Comparison of the pseudo-wave-functions (solid lines) and the corresponding all-electron valence wave functions (dashed lines) for the ground state ($4d^5 5s^1$) of Mo. (b) Comparison of the nonlocal pseudopotential (solid lines) with the ion-core Coulomb potential (dashed line) of Mo.

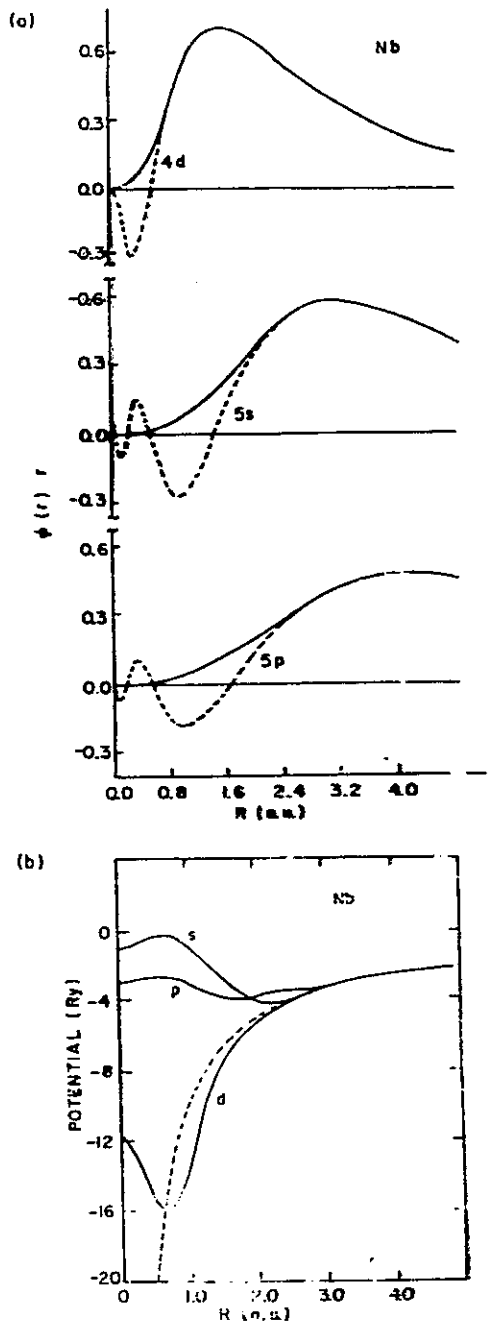

FIG. 2. Pseudopotential for Nb and pseudo-wave-functions in the ground-state configuration ($4d^4 5s^1$).

DENSITY FUNCTIONAL THEORY

KOHN-SHAM EQUATIONS

$$\left[-\frac{\nabla^2}{2} + V_{ion}(\vec{r}) + V_H(\vec{r}) + V_{xc}(\vec{r}) \right] \psi_i(\vec{r}) = \varepsilon_i \psi_i(\vec{r})$$

$$V_{ion}(\vec{r}) = \sum_{\vec{R}_I} V(\vec{r} - \vec{R}_I)$$

$$V_H(\vec{r}) = \int \frac{n(\vec{r}')}{|\vec{r} - \vec{r}'|} d\vec{r}'$$

FOR A GIVEN IONIC CONFIGURATION $\{\vec{R}_I\}$ THE GROUND STATE ENERGY : $\min_{\{\psi_i\}} E[\{\psi_i\}, \{\vec{R}_I\}]$

$$E[\{\psi_i\}, \{\vec{R}_I\}] = 2 \sum_i \int \psi_i^* \left(-\frac{\nabla^2}{2}\right) \psi_i \, d\vec{r} + \int V_{ion}(\vec{r})\, n(\vec{r})\, d\vec{r}$$

$$+ \frac{1}{2} \int \frac{n(\vec{r})\, n(\vec{r}')}{|\vec{r} - \vec{r}'|} d\vec{r}\, d\vec{r}' + E_{xc}[n(\vec{r})] + E_{ion}[\{\vec{R}_I\}]$$

$$n(\vec{r}) = \sum_i f_i |\psi_i|^2$$

SELF-CONSISTENT SOLUTION - ANY SYSTEM

BLOCH'S THEOREM

$$\psi_i^{\vec{k}}(\vec{r}) = \sum_{\vec{G}} C_{i\,\vec{k}+\vec{G}} \exp\left[i(\vec{k} + \vec{G}) \cdot \vec{r} \right]$$

WHEN PSEUDOPOTENTIALS ARE USED.
ADVANTAGE: SITE INDEPENDENT
~ 100 PLANEWAVES PER ATOM, ACCURACY

PROBLEM: EFFORTS GROW RAPIDLY AS THE NUMBER OF ATOMS IN A CELL INCREASES OR WHEN ONE DEALS WITH LOCALIZED ORBITALS

SUPERCELL METHOD

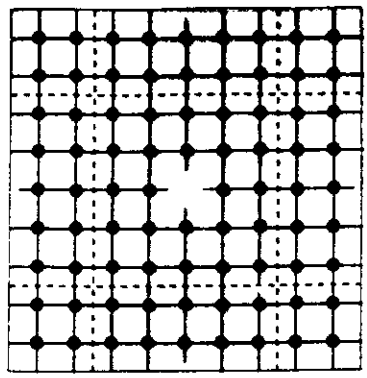

DEFECT

FIG. 2. Schematic illustration of a supercell geometry for a point defect (i.e., vacancy) in a bulk solid. The supercell is the area enclosed by the dashed lines.

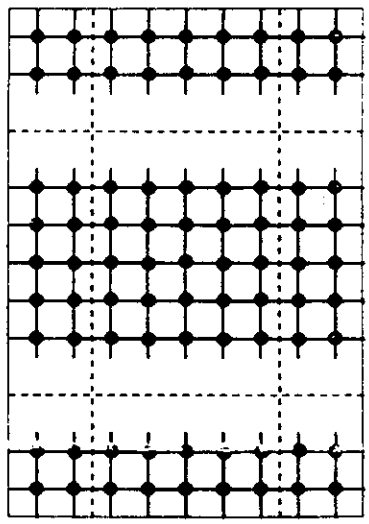

SURFACE

FIG. 3. Schematic illustration of a supercell geometry for a surface of a bulk solid. Same convention as in Fig. 2.

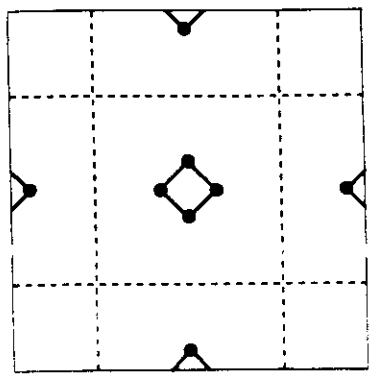

CLUSTER

FIG. 4. Schematic illustration of a supercell geometry for a molecule. Same convention as in Fig. 2.

PERIODIC BOUNDARY CONDITIONS

TOTAL ENERGY CALCULATION
USING
CONVENTIONAL MATRIX DIAGONALIZATION

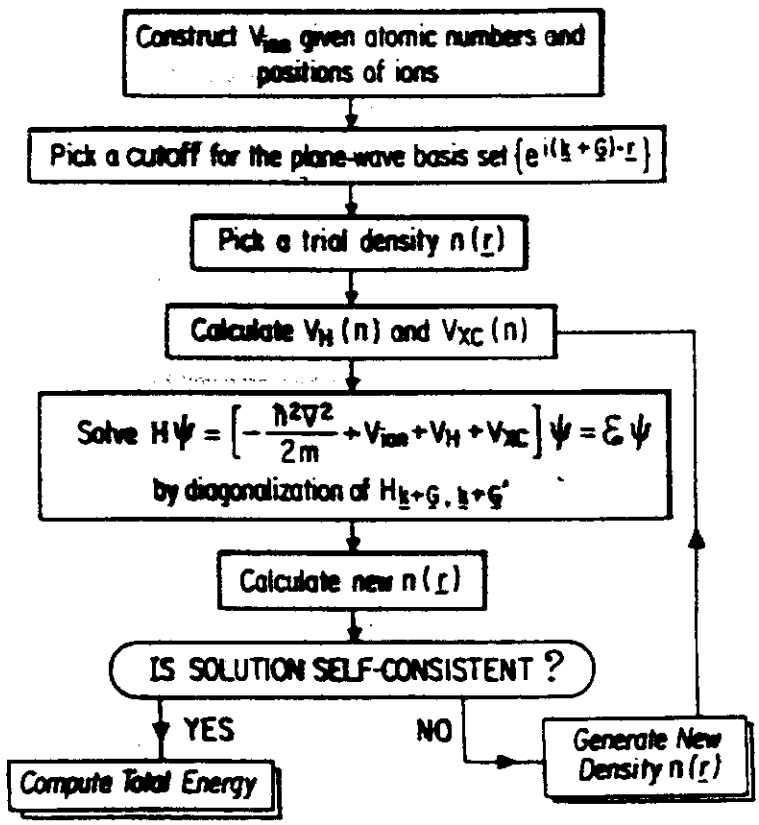

FIG. 7. Flow chart describing the computational procedure for the calculation of the total energy of a solid, using conventional matrix diagonalization.

CAN NOT BE APPLIED TO VERY LARGE SYSTEMS

DIFFICULTIES

LARGE SYSTEMS $t \sim N_A^3$

IONS HAVE TO BE MOVED

DEFECTS

AMORPHOUS

SURFACE RECONSTRUCTION

CLUSTERS ...

IMPORTANT DEVELOPMENT 1985

COMBINED DENSITY FUNCTIONAL MOLECULAR DYNAMICS

SYSTEMS WITH ~ 100 ATOMS

SIMULTANEOUS MINIMIZATION OF ENERGY w.r.t. ELECTRONIC AND IONIC DEGREES OF FREEDOM

FINITE TEMPERATURE STUDIES

Ab initio MOLECULAR DYNAMICS

TREAT $\{\psi_i\}$ AND $\{\vec{R}_I\}$ DYNAMICAL VARIABLES OPTIMIZATION PRO

$$\mathcal{L} = \sum_i \frac{1}{2}\mu \int_\Omega d\vec{r}\, |\dot{\psi}_i|^2 + \frac{1}{2}\sum_I M_I \dot{R}_I^2 - E\left[\{\psi_i\}, \{\vec{R}_I\}\right]$$

(MANY WAYS)

ASSUMPTION: BORN-OPPENHEIMER APPROXIMATION

ψ_i's ORTHONORMAL

$$\int_\Omega d\vec{r}\, \psi_i^*(\vec{r},t)\,\psi_j(\vec{r},t) = \delta_{ij}$$

EQUATIONS OF MOTION

$$\frac{d}{dt}\left\{\frac{\partial \mathcal{L}}{\partial \dot{\psi}_i^*}\right\} = \frac{\partial \mathcal{L}}{\partial \psi_i^*}$$

$$\frac{d}{dt}\left\{\frac{\partial \mathcal{L}}{\partial \dot{\vec{R}}_I}\right\} = \frac{\partial \mathcal{L}}{\partial \vec{R}_I}$$

$$\therefore \quad \mu\ddot{\psi}_i(\vec{r},t) = -\frac{\partial E}{\partial \psi_i^*} + \sum_j \Lambda_{ij}\psi_j(\vec{r},t)$$

$$M_I \ddot{\vec{R}}_I = -\nabla_{\vec{R}_I} E$$

$$\dot{\psi}_i = 0 \quad \Rightarrow \quad \frac{\partial E}{\partial \psi_i^*} = \Lambda_i \psi_i$$

STANDARD PROBLEM

WITH $\psi_i(\vec{r}) = \sum_{\vec{G}} C_{i\vec{G}}\, e^{i\vec{G}\cdot\vec{r}}$ Γ POINT

EOM: $$\mu \ddot{C}_{i\vec{G}} = -\left[\frac{1}{2}|\vec{G}|^2 - \Lambda_i\right] C_{i\vec{G}} - \sum_{\vec{G}'} V^{H}_{\vec{G}-\vec{G}'} C_{i\vec{G}}$$

$$- \sum_{\vec{G}'} V^{xc}_{\vec{G}-\vec{G}'} C_{i\vec{G}'} - \sum_{\vec{G}'} V^{ion}_{\vec{G}\vec{G}'} C_{i\vec{G}'}$$

WORK IN EASY SPACE $\vec{r} \xleftrightarrow[\text{FFT}]{} \vec{G}$-space

VERLET ALGORITHM

$$C_{i\vec{G}}(\Delta t) = 2 C_{i\vec{G}}(0) - C_{i\vec{G}}(-\Delta t) + (\Delta t)^2 \ddot{C}_{i\vec{G}}$$

CALCULATION OF TOTAL ENERGY

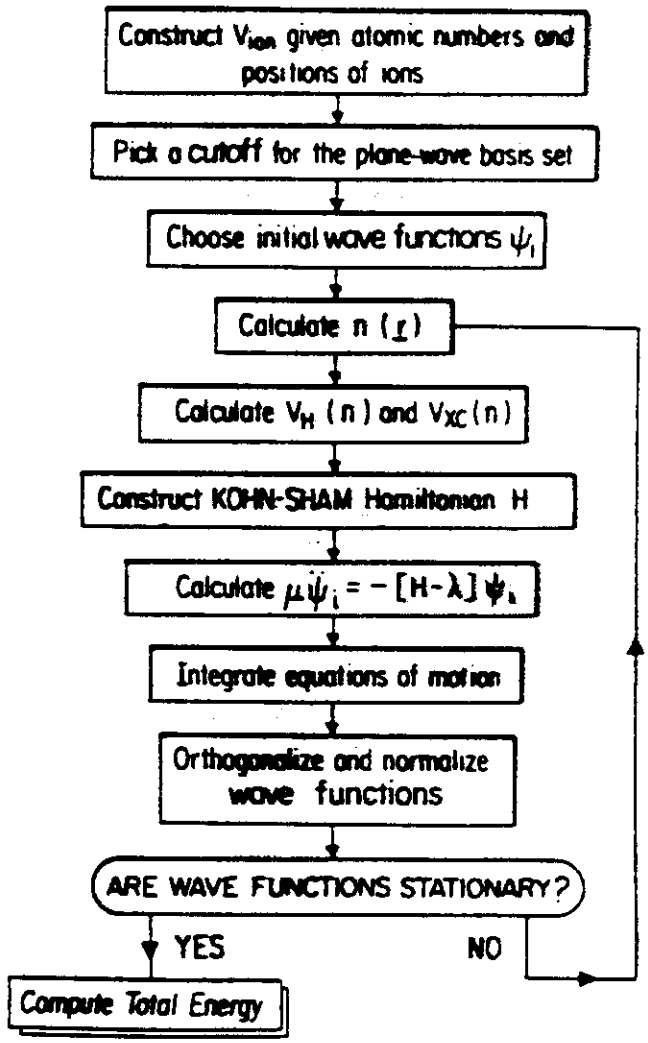

FIG. 11. Flow chart describing the computational procedure for the calculation of the total energy of a solid with molecular dynamics.

DYNAMICS OF IONS:

$$M_I \ddot{\vec{R}}_I = -\frac{\partial E}{\partial \vec{R}_I}$$

$$E = \langle \Psi | H | \Psi \rangle + E^{ion}$$

$$M_I \ddot{\vec{R}}_I = -\frac{\partial}{\partial \vec{R}_I} \left[\langle \Psi | H | \Psi \rangle + E^{ion} \right]$$

$$= -\left[\langle \frac{\partial \Psi}{\partial \vec{R}_I} | H | \Psi \rangle + \langle \Psi | \frac{\partial H}{\partial \vec{R}_I} | \Psi \rangle \right.$$

$$\left. + \langle \Psi | H | \frac{\partial \Psi}{\partial \vec{R}_I} \rangle + \frac{\partial E^{ion}}{\partial \vec{R}_I} \right]$$

IF Ψ IS AN EIGENSTATE OF H

THEN $H\Psi = E^{el}\Psi$

SO $\langle \frac{\partial \Psi}{\partial \vec{R}_I} | H | \Psi \rangle + \langle \Psi | H | \frac{\partial \Psi}{\partial \vec{R}_I} \rangle$

$$= \langle \frac{\partial \Psi}{\partial \vec{R}_I} | E^{el} \Psi \rangle + \langle \Psi E^{el} | \frac{\partial \Psi}{\partial \vec{R}_I} \rangle$$

$$= E^{el} \frac{\partial}{\partial \vec{R}_I} \langle \Psi | \Psi \rangle = 0$$

IF Ψ IS AN EIGENSTATE OF H, THE
ONLY THE EXPLICIT DEPENDENCE
OF E ON $\{\vec{R}_I\}$ NEED TO BE CALCULAT
THE CAR-PARRINELLO DYNAMICS WO
WHEN DEVIATIONS FROM SURFACE
ARE SMALL.

MOTION OF ORBITAL AND IONS

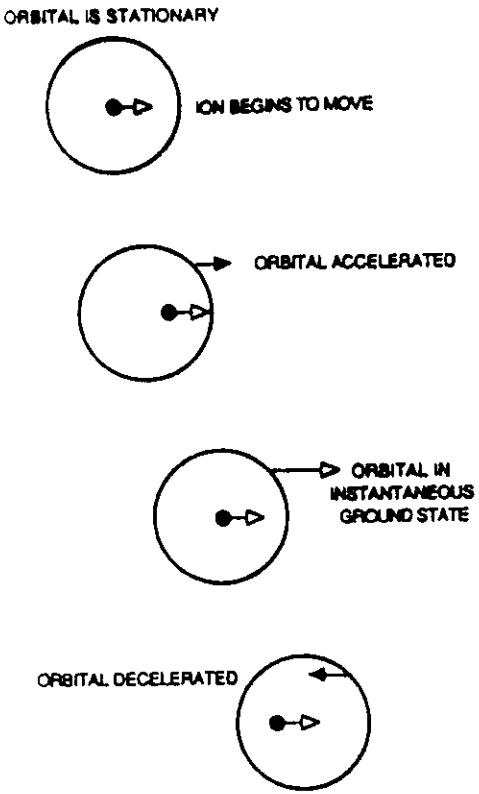

FIG. 23. Schematic illustration of how an orbital will oscillate around a moving ion during a simulation with $\mu\ddot{\psi} = -[H - \lambda]\psi$, as discussed in the text. Velocities and accelerations are designed as open and filled arrows, respectively.

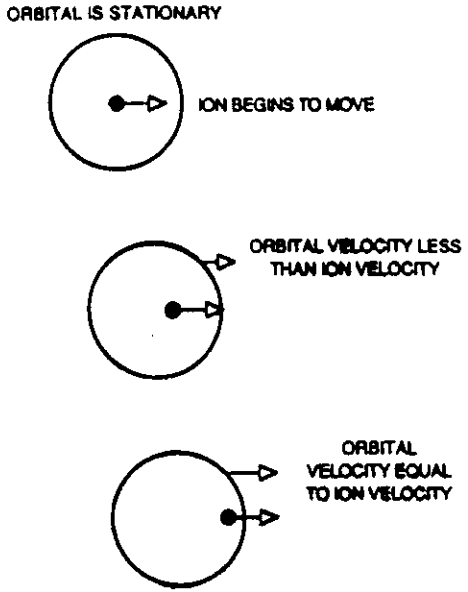

FIG. 24. Schematic illustration of how an orbital will eventually lag behind a moving ion during a simulation with $\mu\dot{\psi} = -[H - \lambda]\psi$, as discussed in the text. Convention the same as in Fig. 23.

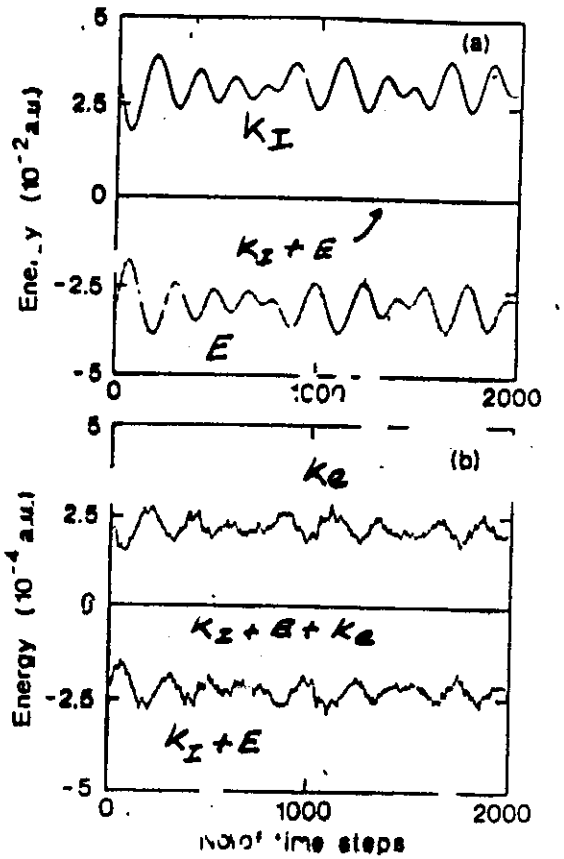

Fig. 3. The time variation of the electronic and ionic energies on a segment of 2000 steps for a run of 16 Si atoms in the diamond structure (see text). K_I (dotted line), $\psi_{i_0}(\{R_I\})$ (dashed-dotted line) and $U_I' = V_I + E$ (full line) are shown in the upper part of the figure, (a), on an energy scale of 10^{-2} a.u. K_e (dotted line), U_I' (dashed-dotted line) and $U_{eI} = U_I' + K_e$ (full line) are shown in the lower part, (b), on an energy scale of 10^{-4} a.u. E, U_I' and J_{eI} are measured relative to the initial value $U_{eI} = -61.62887$ (from Ref. [3]).

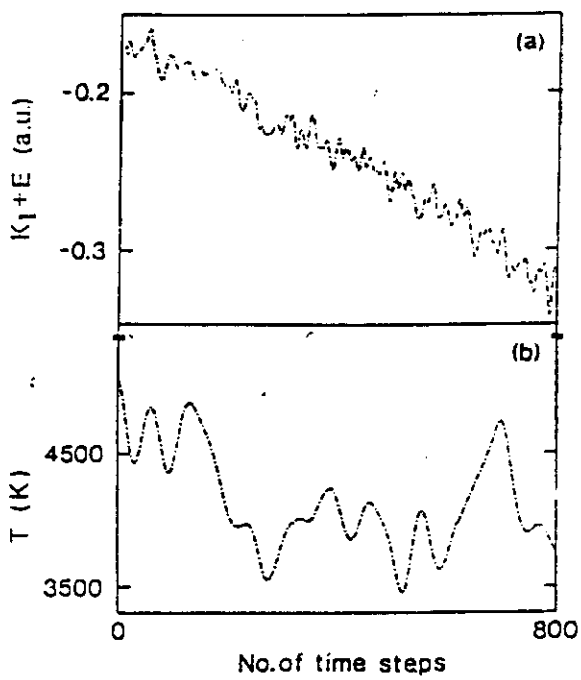

Fig. 4. The time variation of (a) $U_I' = K_I + E$ and (b) the ionic temperature T, on a segment of 800 steps for a run of 54 C atoms in a liquid-like (diffusive) state. The system is metallic (from Ref. [3]).

SIMULATED ANNEALING

SYSTEM IS HEATED TO HIGH ENOUGH TEMPERATURE SO THAT IT BEHAVES LIKE A LIQUID

IT IS THEN COOLED SLOWLY $\sim 10^{15}$ K/s

VARIATION IN $\dot{\psi}$ AND $\dot{\vec{R}}$ ALLOW THE DYNAMICAL SYSTEM TO UNDERGO VARIOUS THERMAL TREATMENTS: ANNEALING, QUENCHING etc.

SIMULATION TIME $\sim$ 1 ps
(COMPARE WITH STANDARD MD $\sim$ 1 ns

$$\sum_i \mu \int_\Omega d\vec{r}\, |\dot{\psi}_i(\vec{r})|^2 + \frac{1}{2}\sum_I M_I \dot{\vec{R}}_I^2 = \frac{3}{2} N k_B T.$$

$\Delta t \sim 10^{-16}$ s DEPENDS UPON THE KINETIC ENERGY OF PLANE WAVES

- $\psi_i^{\vec{k}}(\vec{r}) = \sum_{\vec{G}} C_{i\,\vec{k}+\vec{G}} \exp[i(\vec{k}+\vec{G})\cdot\vec{r}]$
- ONLY $k=0$ POINT
- NORM-CONSERVING PSEUDO-POTENTIALS OF BACHELET et al
- s NON-LOCALITY
- UNIT CELL LARGE ENOUGH SO THAT MINIMAL INTERACTION BETWEEN CLUSTER AND ITS IMAGES
- SMALL CLUSTERS WITH STEEPEST DESCENT $N < 6$
- LARGER CLUSTERS WITH SIMULATED ANNEALING
- LOCAL DENSITY APPROXIMATION